

Proposal for the next E05 run with the $S - 2S$ spectrometer

Tomofumi NAGAE^a (Spokesperson), S. Kanatsuki,^a H. Ekawa,^a T. Nanamura,^a
A. Koshikawa,^a H. Fujioka,^a M. Naruki,^a S. Hasegawa,^b K. Hosomi,^b Y. Ichikawa,^b
K. Imai,^b H. Sako,^b S. Sato,^b K. Tanida,^b J. Yoshida,^b S.H. Hayakawa,^c M. Nakagawa,^c
Y. Nakada,^c T. Akaishi,^c A. Sakaguchi,^c Y. Akazawa,^d M. Fujita,^d R. Honda,^d K. Miwa,^d
H. Kanauchi,^d H. Tamura,^d T. Gogami,^d S.N. Nakamura,^d M. Kaneta,^d S. Nagao,^d
Y. Toyama,^d K. Itabashi,^d K. Aoki,^e E. Hirose,^e H. Takahashi,^e T. Takahashi,^e M. Ukai,^e
T.O. Yamamoto,^e J.K. Ahn,^f S.H. Kim,^f H.M. Yang,^f K.Y. Roh,^f M. Agnello,^g
E. Botta,^{gm} A. Feliciello,^g P. Evtoukhovitch,^h Z. Tsamalaidze,^h J.Y. Lee,ⁱ T. Moon,ⁱ
S. Kimbara,^j T. Hasegawa,^k K. Shirotori,^l M. Yosoi,^l D. Shoukavy,ⁿ L. Tang^{op}

– J-PARC E05 Collaboration –

^a Department of Physics, Kyoto University, Kitashirakawa, Kyoto 606-8502, Japan

^b ASRC, JAEA, Tokai, Ibaraki 319-1195, Japan

^c Department of Physics, Osaka University, Toyonaka, Osaka 560-0043, Japan

^d Department of Physics, Tohoku University, Sendai 980-8578, Japan

^e IPNS, KEK, Tsukuba, Ibaraki 305-0801, Japan

^f Korea University, Seoul 136-713, Korea

^g INFN Sezione di Torino, 10125 Torino, Italy

^h JINR, Dubna, Russia

ⁱ Department of Physics and Astronomy, Seoul National University, Seoul 151-747, Korea

^j Faculty of Education, Gifu University, Gifu 501-1193, Japan

^k Kitasato University, Sagami, Japan

^l RCNP, Osaka University, Ibaraki, Osaka 567-0047 Japan

^m Università di Torino, 10124 Torino, Italy

ⁿ B.I. Stepanov Institute of Physics, National Academy of Sciences of Belarus, Belarus

^o Department of Physics, Hampton University, Hampton, Virginia 23668, U.S.A.

^p Thomas Jefferson National Accelerator Facility (JLab), Newport News, Virginia 23606, U.S.A.

^q Politecnico di Torino, Torino 10129, Italy

(Received December 15, 2017)

The original E05 proposal entitled "Spectroscopic Study of Ξ -hypernucleus, ^{12}Be , via the $^{12}\text{C}(K^-, K^+)$ Reaction" was submitted during the 1st PAC meeting, and had been considered to be the 1st priority experiment among the five Day-1 experiments (E05, E13, E15, E17, E19) in the Hadron Hall. In this document, we update the proposal taking into accounts the present and the near-future beam conditions and the recent progress on Ξ -hypernuclei; in particular with our preliminary analysis in the E05 pilot run.

KEYWORDS: E05, Ξ -hypernucleus, $S-2S$, J-PARC

1. Motivations of E05

1.1 Ξ -N Interaction

One of the important goals of hypernuclear spectroscopy is to establish a modern picture of generalized nuclear force models in relation to quantum chromo-dynamics (QCD) by extending the nucleon-nucleon force in flavor $SU(3)$. The forces between two octet baryons, such as N - N , Y - N , Y - Y , are its subjects. Here the Y stands for a baryon with strangeness, that is a hyperon (Λ , Σ , Ξ). Because

of the short life time (10^{-10} sec.) of the hyperons, it is difficult to carry out Y - N , Y - Y scattering measurements. Therefore, we have been investigating the spectroscopy of hypernuclei to extract the information on the Y - N and Y - Y interactions. For example, the fine structure of p -shell Λ hypernuclei has revealed spin-dependent interactions of Λ - N force [1]. A precious information on the Λ - Λ force was obtained in the ‘‘Nagara’’ event in emulsion [2, 3]. Knowing that the Σ - N force is repulsive on average [4], the last key information is the Ξ - N interaction, which is the major subject in E05 experiment.

In a recent study of Lattice QCD calculations [5], the Ξ - N interaction potentials are available for various $S = -2$ channels, although the pion mass involved in the calculations is still large compared to its physical mass. Such a comparison between theory and experiment in near future would be very much interesting.

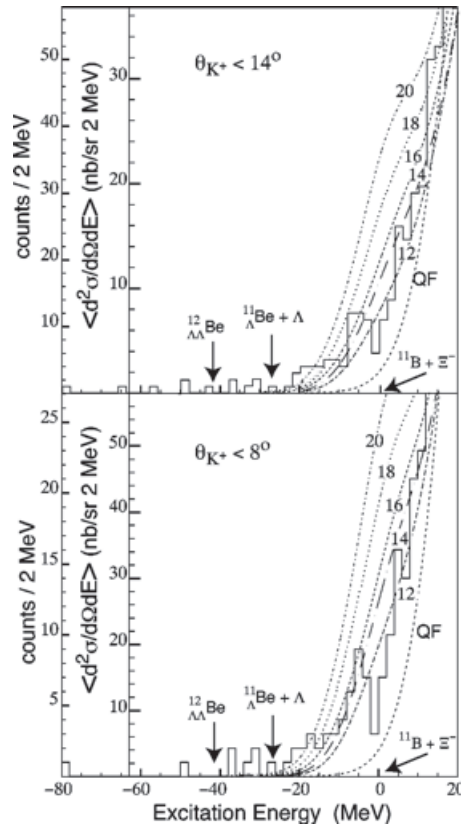


Fig. 1. Excitation-energy spectra from E885 for $^{12}\text{C}(K^-, K^+) X$ reaction for $\theta_{K^+} < 14^\circ$ (top) and $\theta_{K^+} < 8^\circ$ [10]. Theoretical curves for the different Ξ potential depths equal to 20, 18, 16, 14 and 12 MeV were superimposed.

1.2 Hyperon Puzzle

In the nuclear matter at the density of 2–3 times the nuclear saturation density, ρ_0 , the strangeness degrees of freedom should play an essential role. Such a high-density condition is believed to be realized in the core of neutron stars. At such high density, the neutron Fermi energy would become larger than the mass difference between a Λ hyperon ($1115 \text{ MeV}/c^2$) and a nucleon ($939 \text{ MeV}/c^2$) and a lot of strangeness, Λ hyperons, would be created because of the attractive potential, U_Λ felt by the Λ hyperons in high density neutron matter. Thereby, the Fermi pressure would be reduced by

strangeness degrees of freedom. The experimental information on U_Λ was obtained to be 30 ± 1 MeV from the binding energy of heavy Λ hypernuclei up to $^{208}_\Lambda\text{Pb}$ [6].

Another important feature of the strangeness is that s quark has negative charge of $-1/3e$. Therefore the hyperons have negative charge states such as Σ^- and Ξ^- . In the case of nucleons, proton and neutron, with up ($+2/3e$) and $down$ ($-1/3e$) quarks, there are no negatively charged baryons. Thus, from the charge neutrality condition, the number of electrons can be converted to the number of negative hyperons which greatly reduce the electron Fermi energy in the chemical balance of

$$\frac{p_F^e{}^2}{2m_e} + m_e = \frac{p_F^Y{}^2}{2m_Y} + m_Y + U_Y. \quad (1)$$

Here, it is important to know the hyperon potential depths, U_Y . The lightest negative hyperon, Σ^- (1197.4 MeV/ c^2), has strongly repulsive potential of $U_\Sigma \sim +30$ MeV. Therefore, the Σ^- would not appear in neutron stars. The next candidate is Ξ^- (1321.7 MeV/ c^2). At this moment, we have no definite information on the U_Ξ . Therefore, it is awaited to have a good estimate of U_Ξ from the binding energy measurements of the Ξ hypernuclei.

Based on the present knowledge of hypernuclei mentioned above, it is believed that the appearance of strangeness in such high-density nuclear matter is unavoidable and leads to the "Soft" equation of state (EoS). From the softening of the nuclear matter at high density, the maximum mass of neutron stars cannot exceed $1.4 \times M_\odot$. Therefore, recent observations of $2 \times M_\odot$ neutron stars [7, 8] have a serious problem, called "Hyperon Puzzle".

1.3 Experimental Information on Ξ -hypernuclei

The experimental information on Ξ -hypernuclei has been very much limited so far. The missing-mass measurements with the $^{12}\text{C}(K^-, K^+)$ reaction were carried out at KEK [9] and BNL [10], although the statistics and the energy resolution were poor; energy resolution of the former case was $\sigma = 9.5$ MeV and of the latter case was 6.1 MeV. Nevertheless, the E885 experiment observed about 42–67 events in the bound region $20 > B_\Xi > 0$ MeV and claimed evidence of the bound state (Fig. 1). Provided the Woods-Saxon type of the potential form, an initial analysis by BNL E885 group suggested an attractive Ξ potential with a depth of about 14 MeV. It might lead to a bound state at the binding energy of about 4.5 MeV. A reanalysis by Kohno *et al.* suggested almost zero [11] or even a weakly repulsive potential [12].

Recently, KEK E373 group discovered the "Kiso" event [13], as the first evidence of a deeply-bound $\Xi^- - ^{14}\text{N}$ system in the reaction $\Xi^- - ^{14}\text{N} \rightarrow ^{10}_\Lambda\text{Be}$ and $^5_\Lambda\text{He}$. The binding energy was estimated to be 3.87 ± 0.21 MeV, by assuming both $^{10}_\Lambda\text{Be}$ and $^5_\Lambda\text{He}$ are in the ground state, which was definitely larger than the $\Xi^- - ^{14}\text{N}$ atomic binding energy of 0.17 MeV ($2p$ atomic orbit). Please note that the binding energies of the ground state and excited state of $^{10}_\Lambda\text{Be}$ have been updated with the most recent values reported by the JLab E05-115 [14]. Even in the case that the $^{10}_\Lambda\text{Be}$ is in the excited state, the binding energy is 1.03 ± 0.18 MeV. Therefore it seems that a strongly-bound $\Xi^- - ^{14}\text{N}$ state exists, although the binding energy has an ambiguity. There is also an ambiguity from the strong conversion width induced by the $\Xi^- + p \rightarrow \Lambda\Lambda$ process. Therefore, it is difficult to determine the binding energy from a single event.

1.4 Coupling between Ξ -hypernuclei and double- Λ hypernuclei

There could exist couplings between two systems of $S = -2$, Ξp and $\Lambda\Lambda$, through a strong conversion process of $\Xi N \rightarrow \Lambda\Lambda$ [15]. Their masses are separated only by 28.62 MeV in vacuum (Fig. 2). Depending on the coupling strength, a part of the production strength of Ξ -hypernucleus state is used to excite the excited levels of double- Λ hypernucleus. Further, the energy levels of two-states would be attracted to make their separation narrower (of the order of 100 keV). Therefore, the coupling

strength is determined with the production cross section ratio between the two states and the energy separation of two states.

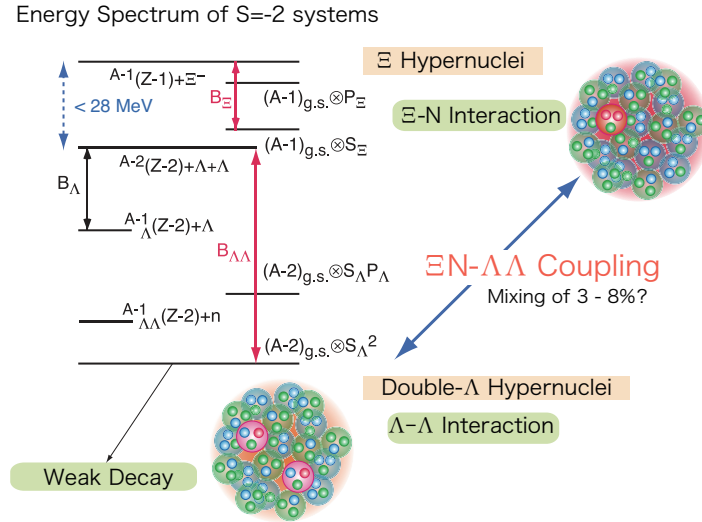


Fig. 2. Schematic energy spectrum of $S = -2$ hypernuclei. The Ξ hypernuclei and double- Λ hypernuclei are only separated by 28.62 MeV, and couple through the $\Xi^- p \rightarrow \Lambda\Lambda$ interaction.

2. History of E05 –Spectrometers

We, originally, planned to construct the SKS+ spectrometer system by adding a small dipole magnet in front of the SKS spectrometer as shown in Fig. 3. However the primary beam intensity from the J-PARC main ring (MR) was significantly lower than expected in the early stage of the MR beam commissioning. Therefore, we tried to increase the acceptance of the spectrometer to compensate the low primary beam intensity; at the same time we tried to improve the momentum resolution. Fortunately, in 2011 we succeeded to obtain a grant budget of about 3 million dollars to construct a new spectrometer dedicated to the study of the (K^-, K^+) reaction. We call it “Strangeness -2 Spectrometer (S-2S)”. As shown in Table I, the performance of the $S-2S$ supersedes that of SKS+ in all aspects. Based on this change, we presented a revised run plan upon the PAC request considering the realistic beam conditions, during the 13th PAC meeting in January, 2012.

Performance	SKS+	$S-2S$	SKS
Acceptance (msr)	30	55	110
Missing-mass resolution (FWHM)	3 MeV	$\lesssim 2$ MeV	6 MeV
Magnet Configuration	DD	QQD	D

Table I. Comparison of two spectrometers: SKS+ in the original proposal and $S-2S$. In the last column, the SKS performance in the pilot run is listed for comparison.

In this situation, we requested an E05 pilot run for the $^{12}\text{C}(K^-, K^+)$ reaction at 1.8 GeV/c by using the existing SKS spectrometer, at the 19th PAC meeting in December, 2014. While the beam power of the primary beam from MR was only 39 kW, the large acceptance of the SKS (please refer to

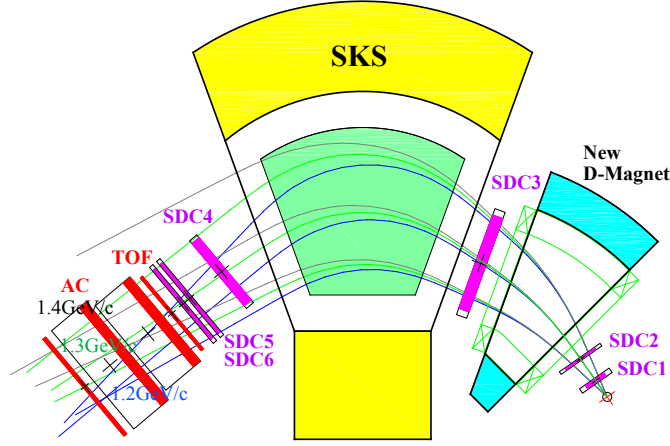


Fig. 3. Schematic view of the E05 setup, SKS+, in the original proposal.

Table I.) would make it possible to observe the ${}_{\Xi}^{12}\text{Be}$ hypernucleus with a moderate energy resolution of 6 MeV. This was a last chance to use the SKS at the K1.8 beam line. Here, we summarize the specifications of the three spectrometers in Table I.

3. E05 pilot run on ${}^{12}\text{C}(K^-, K^+)$ reaction at 1.8 GeV/c with SKS

We have carried out a pilot run of the J-PARC E05 experiment at the K1.8 beam line of J-PARC hadron experimental hall, from October 26 to November 19 in 2015. The typical K^- beam intensity at 1.8 GeV/c was $6 \times 10^5 K^-$ per spill (2.2-sec. beam duration every 5.52 seconds) with a primary proton beam power of 39 kW. The K^-/π^- ratio was about 0.8. We took data using a 9.36-g/cm² nat-C target for about 10 days and a 9.54-g/cm² CH₂ target for about 2 days. The CH₂ target was used for the $p(K^-, K^+)\Xi^-$ reactions at five different incident momenta between 1.5 and 1.9 GeV/c. The total number of K^- 's irradiated on targets amounted to 100 G.

The experimental setup of the E05 pilot run is shown in Fig. 4. In the upstream part of the K1.8 beam line, we have a double-stage electrostatic separator system, and the K^- beam was finally selected through a mass slit (MS2). The incident K^- beam was defined with two sets of plastic scintillation counters (BH1 and BH2) and an aerogel Čerenkov counter (BAC) to suppress π^- 's at the on-line trigger level. The beam momentum was analyzed track by track with the tracking detectors (BFT, BC3 and BC4). The beam line spectrometer was composed of 4 quadrupole magnets (Q10-Q13) and one dipole magnet (D4). The design momentum resolution of the spectrometer was $\Delta p/p \sim 5 \times 10^{-4}$ (FWHM).

The outgoing K^+ was momentum analyzed with the SKS spectrometer with four sets of drift chambers (SDC1-4). In the pilot run, the SKS central momentum was set at about 1.3 GeV/c covering about 110 msr. The momentum resolution of the SKS was $\Delta p/p \sim 3 \times 10^{-3}$. These are great advantages of the SKS compared with the spectrometers used for the (K^-, K^+) reaction in the past.

The particles detected in the SKS were identified with a time of flight measured with a plastics scintillation counter wall of "TOF" correcting with the flight path and momentum obtained from the tracking chambers. The aerogel Čerenkov counter wall "AC" was installed to suppress pions in the trigger level, and the "Lucite Counter (LC)" for suppression of protons.

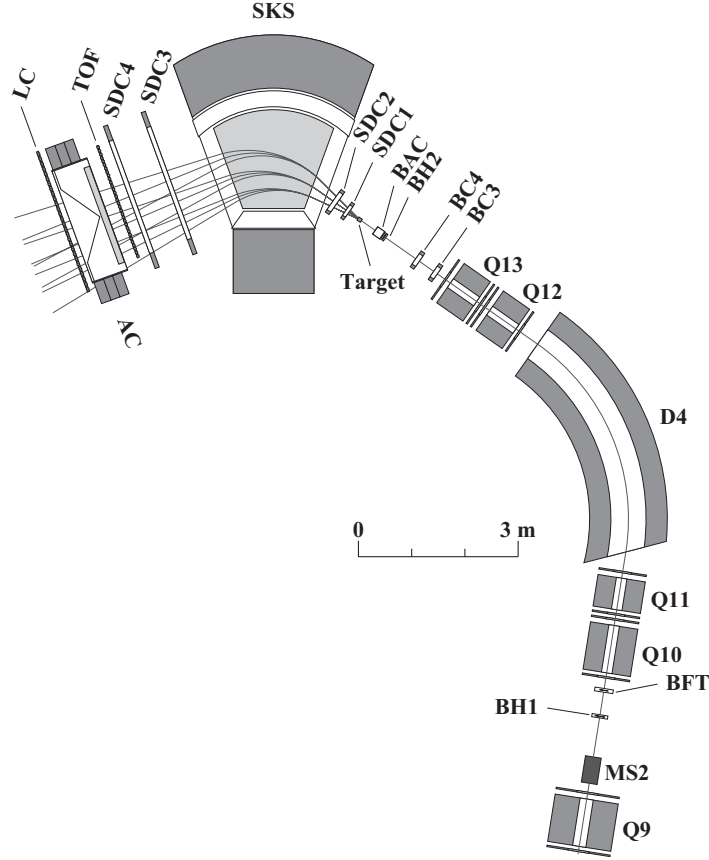


Fig. 4. A schematic view of the experimental setup during the E05 pilot run.

3.1 Analysis for the $p(K^-, K^+)\Xi^-$ reaction

The overall energy resolution was evaluated with the peak for the $p(K^-, K^+)\Xi^-$ reaction at 1.8 GeV/c as shown in Fig. 5, and was confirmed to be 5.4 MeV (FWHM). It is a factor of two better with respect to the 10 MeV of the BNL E885 for proton target. In the Carbon kinematics, the BNL E885 resolution was estimated to be 14 MeV, while our estimate is about 6 MeV which was dominated by the target energy loss straggling. Absolute energy scale of the (K^-, K^+) missing mass was adjusted with this peak position. About 6,000 Ξ^- 's were identified per day.

The incident momentum dependence of the forward cross sections of the $K^- + p \rightarrow K^+ + \Xi^-$ reaction was obtained at 1.5, 1.6, 1.7, 1.8 and 1.9 GeV/c. The statistics at each momentum was more than about 20 times of the statistics of the old bubble chamber data. At 1.8 GeV/c, the statistics was about 100 times to obtain the angular distribution in detail. In a preliminary analysis, we have confirmed with improved statistics that the relative strengths of the cross sections peaks at about 1.8 GeV/c (Fig. 6) as suggested by Dover and Gal [16].

3.2 Analysis for the $^{12}\text{C}(K^-, K^+)\Xi^-$ reaction

The missing mass spectrum of the $^{12}\text{C}(K^-, K^+)\Xi^-$ reaction is shown in Fig. 7-a) as a function of negative values of binding energy (B.E.) of Ξ^- in ^{11}B . Owing to the large momentum acceptance of the SKS, we were able to obtain the spectrum in a wide energy range. The largest part of the spectrum comes from the quasi-free production of Ξ 's peaking at about 110 MeV, while the contribution of Ξ^* can be seen in the higher energy region. Due to the large momentum transferred to Ξ (~ 550 MeV/c) in this reaction, the sticking probability is small, so that there are very few events in the bound region

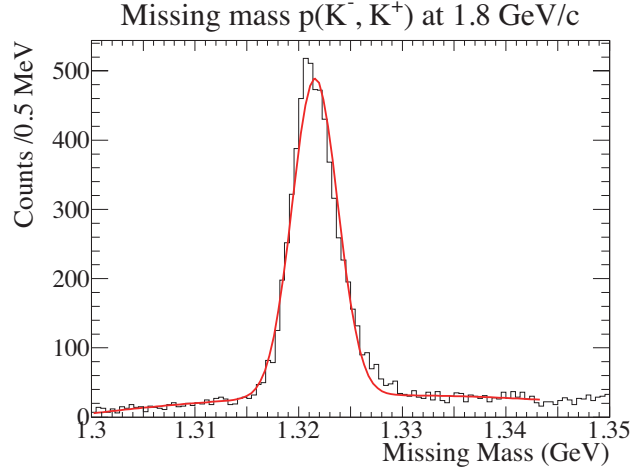


Fig. 5. Missing-mass spectrum for the $p(K^-, K^+)X$ reaction at 1.8 GeV/c obtained with a CH_2 target. The peak corresponds to the reaction on proton and the continuous background below the peak is the contribution of quasi-free Ξ^- production from ^{12}C .

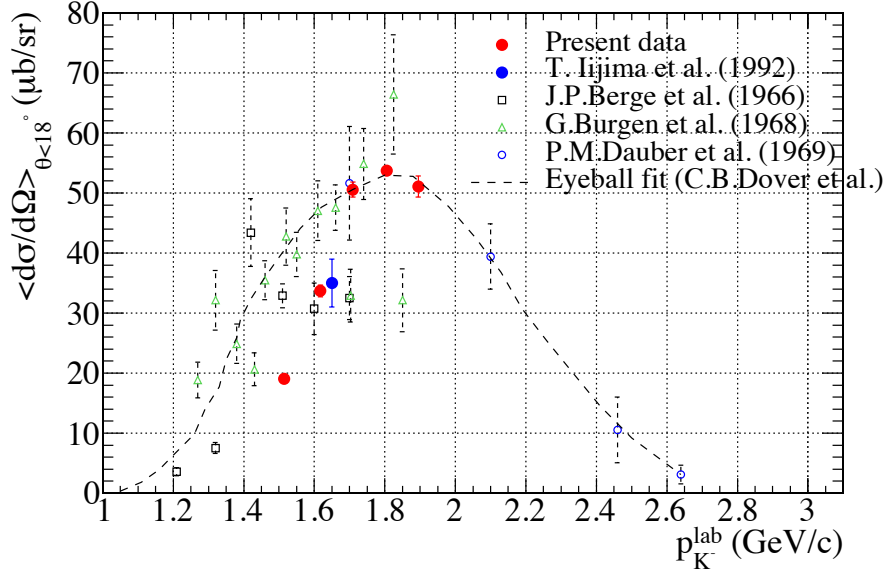


Fig. 6. The incident momentum dependence of the differential cross section of the $p(K^-, K^+)\Xi^-$ reaction at forward angles. The present data is shown in red together with other old data.

(-B.E. < 0) in this vertical scale. A large shift of the quasi-free peak is also due to the large momentum transfer.

Next we magnify the view in the bound region as indicated in Fig. 7-a) as a dashed oval, and we plot it in Fig. 7-b). Here, there should be no physical processes with a binding energy value larger than about 40 MeV (-B.E. ≤ -40 MeV), where the ground state of $^{12}_{\Lambda\Lambda}\text{Be}$ exists. Therefore, we think these

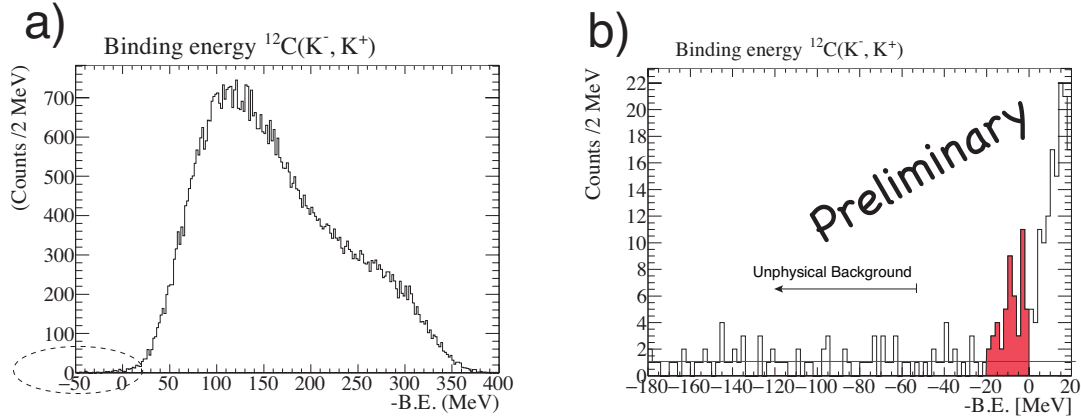


Fig. 7. Missing-mass spectra for the $^{12}\text{C}(K^-, K^+)X$ reaction at 1.8 GeV/c. a) in a wide energy range, and b) a close-up view near the binding energy threshold indicated with a dashed oval in a).

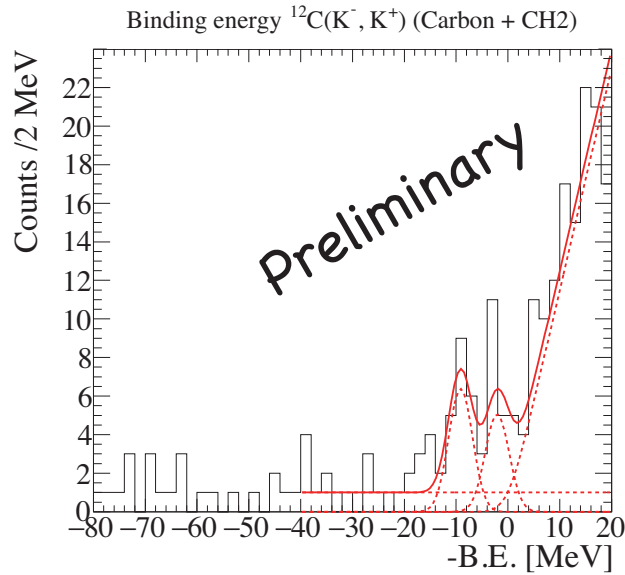


Fig. 8. Missing-mass spectrum for the $^{12}\text{C}(K^-, K^+)X$ reaction at 1.8 GeV/c near the binding energy threshold fitted with two gaussian peaks. The width was fixed at 6 MeV (FWHM).

events in this region should be the background, mostly coming from Kaon decay-in-flight and having almost flat distribution (1.08 counts/ 2 MeV). Then, we observed a significant event excess of about 55 events in the binding energy region between 0 and 20 MeV ($-20 \text{ MeV} \geq -\text{B.E.} \geq 0 \text{ MeV}$) shown in red in Fig. 7-b). This is the same level of statistics obtained by the BNL E885 (42-67 events). Above the binding threshold ($-\text{B.E.} \geq 0 \text{ MeV}$), we clearly see a rise for the quasi-free production.

The momentum acceptance of the SKS corresponding to this energy region is almost flat. We, therefore, tried a fit to the spectrum assuming there exist two gaussian peaks in the bound region and a quasi-free component as a straight line convoluted with the detector energy resolution of 5.4 MeV. We also assumed a flat background component as suggested from the Fig. 7-b). The fitting result is shown in Fig. 8. The red solid line is the fit where the dotted lines show each component. The peak positions were obtained to be about 9 MeV and 2 MeV. If this is the case, the potential depth of the Ξ

in $A = 12$ must be deeper than 14 MeV.

Alternative idea could be that there exists one broad structure in the bound region; assuming such a fit model the width was about 16 MeV and the peak position was still deep at around 7 MeV. Such a large width is not expected in Ξ hypernuclei, and it is statistically significant of the two peak structure. If the width is large, it means that the coupling through $\Xi^- p - \Lambda\Lambda$ is very strong.

4. Experimental Setup with S-2S Spectrometer

In this proposal, we propose to use the $S-2S$ spectrometer for the $^{12}\text{C}(K^-, K^+)$ reaction as in the E05 pilot run which we described the analysis results. A schematic layout of the $S-2S$ spectrometer for the J-PARC E05 experiment is shown in Fig. 9. The K^- beam at 1.8 GeV/c available at the K1.8 beam line is used for the production of Ξ hypernuclei. The production yield of the Ξ^- in the $K^- + p \rightarrow K^+\Xi^-$ reaction has a maximum at 1.8 GeV/c in the forward region, which has been confirmed also in the pilot run with two orders of magnitude better statistics. The incident momentum is analyzed with a beam line spectrometer system composed of $QQDQQ$ in the K1.8 beam line of the J-PARC hadron experimental hall. The momentum resolution is designed to be 3.3×10^{-4} (FWHM). We use the same detector system as in the pilot run listed in Table II.

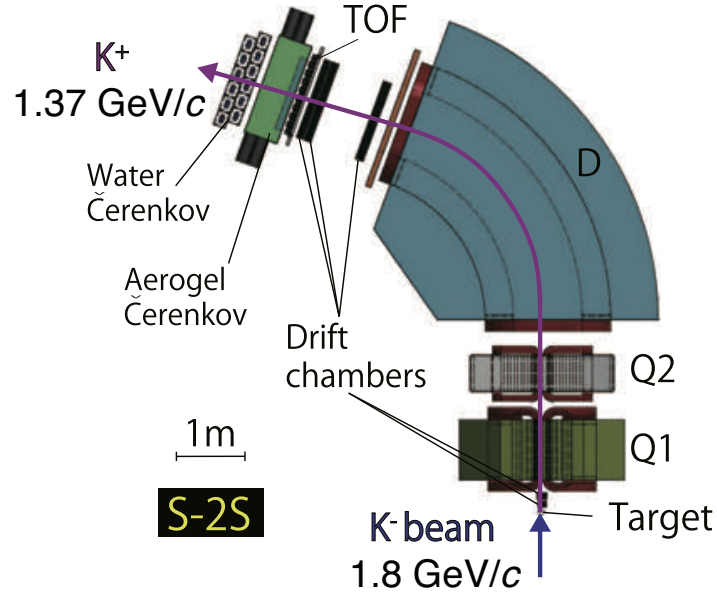


Fig. 9. Schematic view of the S-2S spectrometer system.

Name	configuration	effective area (mm ²)	# of signal channels
BFT	xx'	160×80	160×2
BDC3,4	xx'uu'vv' ×2 sets	192×150	64 x 6 x 2
BH1	11 segments	170×66	11×2
BAC	2 segments	100×100 ×50	4
BH2	7 segments	145×60	7×2

Table II. Specifications of the detectors in the K1.8 beam line.

The K^+ 's scattered at forward angles of $\theta_{K^+} \lesssim 20^\circ$ from the (K^-, K^+) reaction are momentum analyzed with the S -2 S spectrometer. The S -2 S is composed of two quadrupole magnets and one dipole magnet (QQD). The first quadrupole magnet focuses the particles in vertical, and the next one in horizontal. A large aperture of the two quadrupole magnets keeps the solid angle as large as 55 msr as shown in Fig. 10. The bending angle for the central momentum of the dipole magnet is 70 degrees at 1.37 GeV/c. The specifications of the magnet are listed in Table III. The momentum acceptance of the S -2 S ranges from 1.2 to 1.6 GeV/c with the solid angle acceptance larger than ~ 20 msr. The K^+ 's decay in flight, so that the flight length is kept as short as 9 m with a survival rate of 40%. The momentum resolution of the S -2 S is estimated from a simulation and found to be 5.5×10^{-4} (FWHM) (Fig. 11). The S -2 S spectrometer is a similar spectrometer with the HKS constructed at JLab [18]. The momentum resolution was realized to be 2×10^{-4} (FWHM) at 1.2 GeV/c. Due to a large background in front of the HKS, they did not have any tracking detectors in the front section. Thus they needed careful calibrations putting a sieve slit collimator to limit the trajectories. In the case of S -2 S , we have tracking detectors in front of the S -2 S . So, we don't need this calibration.

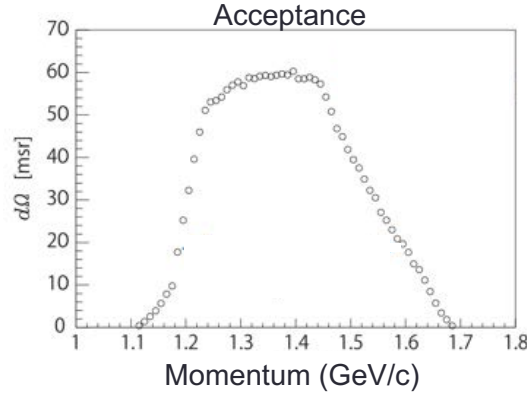


Fig. 10. Acceptance of the S -2 S spectrometer as a function of momentum. The momentum for the Ξ -hypernuclei bound states production corresponds to ~ 1.37 GeV/c.

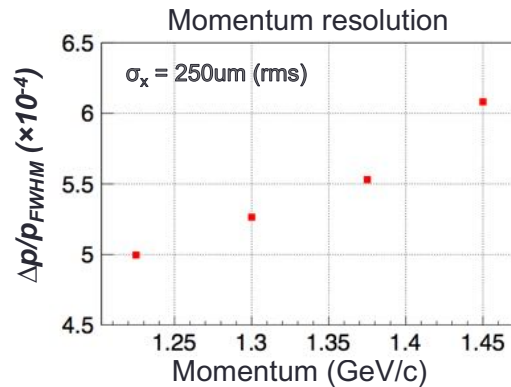


Fig. 11. Momentum resolution of the S -2 S spectrometer in FWHM assuming that the position resolution of the tracking detectors are $250 \mu\text{m}$ in r.m.s. as a function of momentum.

The K^+ trigger signals are generated with a time-of-flight scintillation counter (TOF), an aerogel

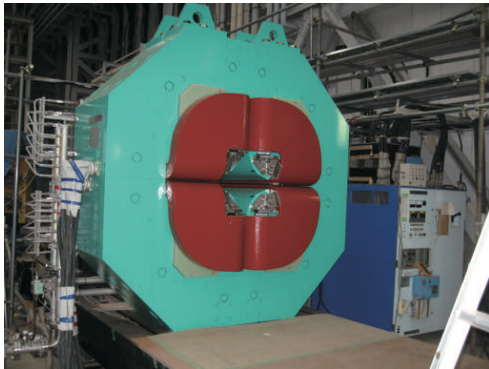
Čerenkov counter (AC: refractive index $n=1.055$) for π^+ veto, and a water Čerenkov counter (WC: $n=1.33$) for proton veto [17], as $TOF \otimes \overline{AC} \otimes WC$. The particle identification is carried out with the TOF counter in off-line analyses by correcting the flight path and momentum obtained from the tracking in $S - 2S$.

	Q1	Q2		D1
Field Gradient (T/m)	8.72	5.0	Field Strength (T)	1.5
Aperture (cm)	31	36	Pole Gap (cm ²)	32×80
Weight (ton)	37	12	Weight (ton)	86

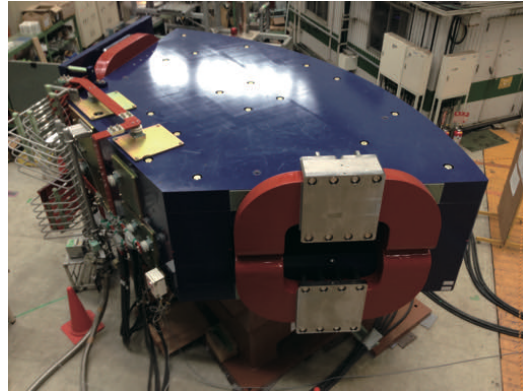
Table III. Specifications of the magnets for the $S-2S$.

4.1 Construction status of the $S-2S$ Spectrometer

The $S-2S$ spectrometer system is now under construction. All the magnets were already constructed (see Fig. 12); Q1 in March 2013, Q2 in March 2014, and D1 in May 2015. The basic performance of the magnets (Table III) was demonstrated safely.



(a) Q1



(b) D1

Fig. 12. Pictures of the (a) Q1 and (b) D1 magnets of the $S - 2S$ spectrometer system.

In order to analyze the K^+ momentum, the magnetic-field map of the $S-2S$ system is necessary. Since the magnetic field measurement with three magnets in their regular positions is difficult, we have measured the field map for each magnet separately. These measured field maps are compared with the calculated field maps by using a three-dimensional finite-element method Opera3D/TOSCA. By optimizing the $B-H$ curve for the irons, we have succeeded to reproduce the Q1 magnetic field within an accuracy of ± 20 Gauss (Fig. 13). Reproducing the field map of each magnet, the field map of the three-magnet system will be calculated with the same code by placing all the three magnets. Of course, this will be a starting point of the field map to be used for momentum analyses in the $S-2S$. We need to optimize the field map by using the $K^- + p \rightarrow K^+ + \Xi^-$ events as the calibration source.

The detector parts of the $S - 2S$ system are also almost ready for installation (Fig. 14). We have developed a water Čerenkov detector for the $S - 2S$ to reduce the proton trigger background by one order of magnitude. The aerogel Čerenkov detector is expected to reject π^+ 's more than 99.7%. The

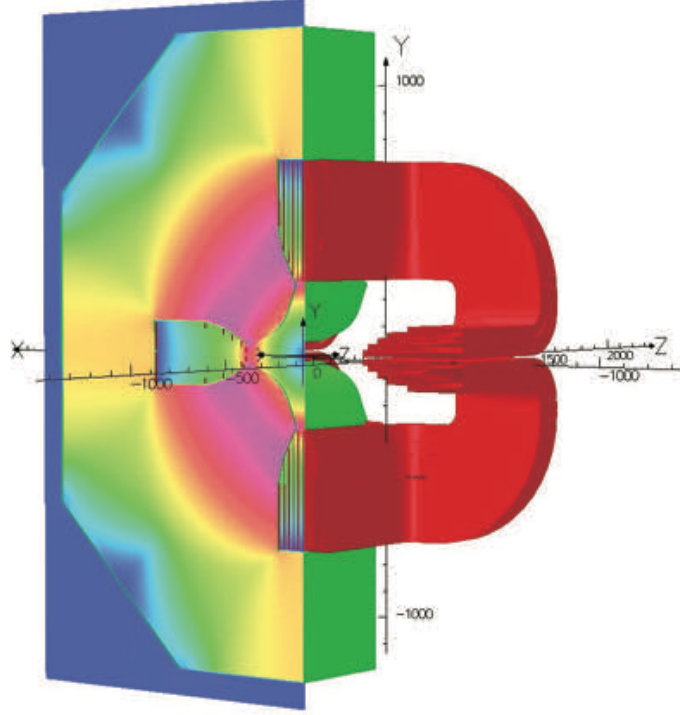


Fig. 13. Simulated magnetic-field map of the Q1 magnet of the S -2 S spectrometer system.

TOF counter is also ready for installation. Several drift chambers need maintenance and the front-end electronics should be fabricated in a year or so.

Name	configuration	effective area (mm ²)	# of signal channels
SDC1	xx'uu'vv'	394×264 × 6 planes	64 ×6
SDC2	uu'vv'	160×300 × 6 planes	44 ×4
SDC3	xx'yy'	1200×900	448
SDC4-5	xx'yy'	1200×1200	128×4
TOF	18 segments	1192×600	18×2
AC	1 box	1400×1400	30 PMTs
WC	12 segments	1450×690	12×2

Table IV. Specifications of the detectors in the S – 2 S .

We plan to install the S -2 S system in the K1.8 beam line in 2019. We hope to have a better intensity of the K^- beam achieved in a pilot run of the J-PARC E05 in 2015. At that time, the K^- intensity was 6×10^5 / 5.52 seconds with the primary proton beam power of 39 kW. We observed about 40 events of signals for 10 days of data taking.

5. Run Plan of E05 with S-2S

Purpose of the Next Run

After the preliminary results from the E05 pilot run, these are the main purpose of the E05 new measurement with S -2 S in 2-MeV missing-mass resolution;

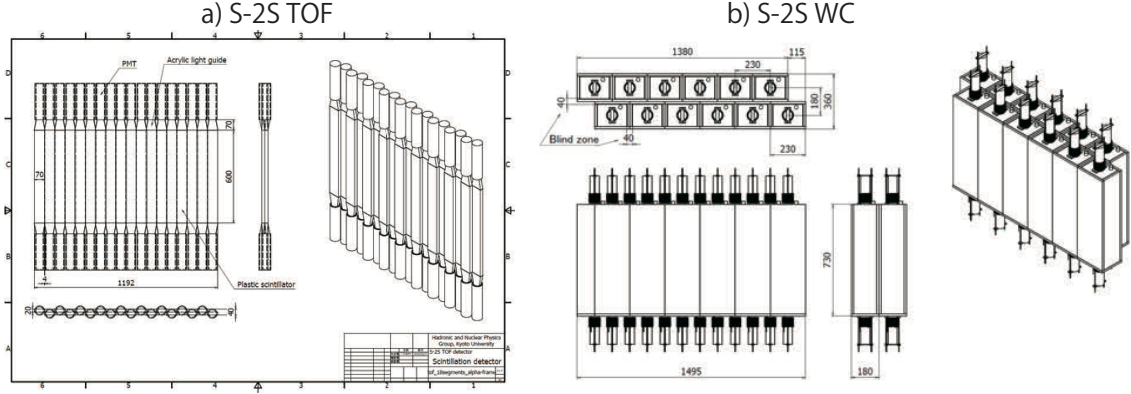


Fig. 14. Schematic drawings of the TOF and WC counter walls for *S-2S* .

Run Conditions	Pilot Run	Next physics Run
K^- intensity (M/spill)	0.6	1.31
MR beam power (kW)	39	85
Spill cycle (s)	5.52	4.7
Target thickness (g/cm^2)	9.3	10
Spectrometer acceptance (msr)	110	55
Missing-mass resolution (FWHM)	6 MeV	<2 MeV
Signal events/days of run	40/10 days	~110/20 days

Table V. Run conditions in the pilot run and the expected condition for the E05 physics run with *S-2S* for $^{12}C(K^-, K^+)_{\Xi}^{12}Be$ reaction at 1.8 GeV/c.

- (1) Separation of two peaks, if existed, about 7-MeV apart with a good energy resolution of 2 MeV (FWHM),
- (2) Measurement of the width of the peak(s).

The energy resolution of 2 MeV enables us to separate the ^{11}B core excited states of which excitation energies are about 2 MeV. So, our measurement will be robust for any fine structures in this mass-number region. The largest binding energy state gives us the ground state energy lower limit with a precision of 0.2 MeV, which is related to the real part of the potential $Re(U_{\Xi})$. The width of the peak might be less than a few MeV if we observed two peaks in the bound region. On the other hand, if we observed one broad peak, the peak width should be larger than 10 MeV, so that the width could be measured easily, and we could obtain the information of imaginary part of the potential, $Im(U_{\Xi})$, with a precision better than 1 MeV.

Based on the results of the pilot run, we can surely estimate the yield of the ^{12}Be bound states in the case of *S-2S*, which has 55-msr solid-angle acceptance corresponding to a half of the SKS acceptance of 110 msr. The run conditions are summarized in Table V.

MR beam power

The beam power from the main ring (MR) to the Hadron Experimental Hall is limited by the production target (T1) for secondary beams. At the time of the E05 pilot run, it was 39 kW, and produced 600 k K^- per spill at 1.8 GeV/c. The present T1 target can be used up to 50 kW. However not more than that. At this moment we have a design of new T1 target made of Au which could sustain up to 85 kW. It will increase the K^- intensity by more than a factor of 2 (2.18). In addition, we would like to shorten the operation cycle of the MR from the present 5.52 sec. to 4.7 sec. or less.

It corresponds to a 100-kW operation of the MR. Even in this case the instantaneous beam rate is $0.6 \text{ M} \times (85/39) / 1.7 \text{ sec.} = 0.77 \text{ M/sec.}$ which is well below the beam rate assumed in the original proposal, $1.4 \text{ M} / 0.8 \text{ sec.} = 1.75 \text{ M/sec.}$

Active Target

We are going to use a 10 g/cm^2 thick target of fiber scintillators. We will use $\phi 3 \text{ mm}$ scintillation (Saint-Gobain, ®BCF-10SC) to make the net target size of $5\text{cm}[\text{H}] \times 10\text{cm}[\text{W}] \times 10 \text{ cm}[\text{T}]$. One unit of the fiber target is composed of 4 (xx'yy') planes of 100 fibers; we have 9 units along the beam direction so that about 900 fibers in total (Fig. 15). The thickness is almost the same with that for the pilot run. Thus, without any corrections for target energy-loss straggling the achieved energy resolution would be 6 MeV (FWHM) as in the pilot run. Here, we will read out the pulse height of each scintillation fiber via MPPC with EASIROC modules. Thereby we can correct the energy loss event by event with the energy loss observed in each fiber along the particle track. Thus we can keep the energy resolution as good as $\sim 1.5 \text{ MeV}$ (FWHM) with a thick target.

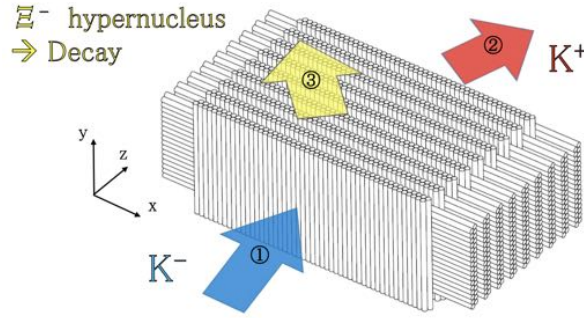


Fig. 15. A conceptual design of the active target made of $\phi 3 \text{ mm}$ scintillation fibers.

We have performed a beam test at RCNP, Osaka, to investigate the energy resolution of each fiber scintillator. The Grand Raiden Spectrometer was used to measure the energy loss in each fiber for a beam particle by particle. The proton beam energy was 65 MeV, and typical energy loss in the $\phi 3 \text{ mm}$ fiber was $\sim 3 \text{ MeV}$. The momentum resolution of the Grand Raiden was negligibly small. The light output from a fiber was about 640 photons and was compared with the energy loss measured with the Grand Raiden. We found the energy resolution of the fiber was about 5% (in σ) (Fig. 16). In the case of $1.4 \text{ GeV}/c \text{ K}^-$, the mean energy loss in the fiber is 0.7 MeV and the energy resolution would be about 6%. According to our simulation, with this energy resolution of energy loss correction we could reach the overall mass resolution of 2 MeV with 10 g/cm^2 thick target.

The hypernuclear missing-mass, M_{Ξ} , is defined as

$$M_{\Xi} = \sqrt{(E_{K^-} + M_A - E_{K^+})^2 - p_{K^-}^2 - p_{K^+}^2 + 2p_{K^-} \cdot p_{K^+} \cos \theta}. \quad (2)$$

From this equation, the missing-mass resolution is expressed with the measurement errors of Δp_{K^-} , Δp_{K^+} , and $\Delta \theta_{KK}$, as

$$\Delta M_{\Xi}^2 = \left(\frac{\partial M}{\partial p_{K^-}} \right)^2 \Delta p_{K^-}^2 + \left(\frac{\partial M}{\partial p_{K^+}} \right)^2 \Delta p_{K^+}^2 + \left(\frac{\partial M}{\partial \theta_{KK}} \right)^2 \Delta \theta_{KK}^2 + \Delta E_{straggle}^2, \quad (3)$$

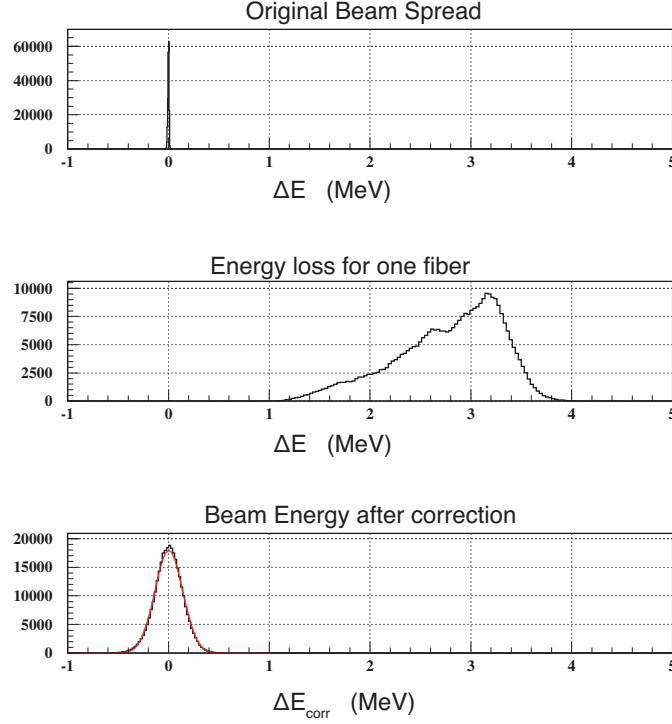


Fig. 16. Results of the RCNP test run for the fiber scintillator. Top) Beam energy spread of 65-MeV proton beam, Middle) Energy loss distribution measured with the Grand Raiden spectrometer for a $\phi 3$ mm scintillating fiber (Widely distributed due to energy loss position dependence and straggling.), Bottom) After correction by using the fiber light output. The width gets narrower.

Conditions	$\left(\frac{\partial M}{\partial p_{K^-}}\right) \Delta p_{K^-}$	$\left(\frac{\partial M}{\partial p_{K^+}}\right) \Delta p_{K^+}$	$\left(\frac{\partial M}{\partial \theta_{KK}}\right) \Delta \theta_{KK}$	$\Delta E_{\text{straggle}}$ (thickness)	ΔM
Designed	0.84 MeV	0.62 MeV	0.04 MeV	1 MeV (3 g/cm ²)	1.45 MeV
Next run (Active)	1.67 MeV	0.62 MeV	0.04 MeV	0.9 MeV (10 g/cm ²)	2 MeV
Next run (Normal)	1.67 MeV	0.62 MeV	0.04 MeV	2.4 MeV (8 g/cm ²)	3 MeV
Pilot run	1.67 MeV	3.74 MeV	0.04 MeV	3 MeV (10 g/cm ²)	5.1 MeV

Table VI. Contribution of each term for the missing-mass resolution in each run condition. Top) Design goal of the S - $2S$ assuming the beam line spectrometer has $\Delta p/p = 5 \times 10^{-4}$, 2nd) Next E05 run with an active target, 3rd) Next E05 run with a normal target without target energy-loss correction, and Bottom) An estimate for the E05 pilot run.

where the $\Delta E_{\text{straggle}}$ is the error due to the energy-loss straggling in the target. The contribution of each term and the missing-mass resolution with a specific target thickness is listed in Table VI. Here, the momentum resolution of the K1.8 beam line spectrometer is assumed to be 5×10^{-4} in the ‘‘Designed’’ column, while it is assumed to be 1×10^{-3} in other run conditions, which was estimated in the K1.8 experiments with SKS. Please note the momentum resolution of the SKS in the previous J-PARC experiments was 3×10^{-3} so that the overall momentum resolution be limited by the SKS resolution. Therefore, we hope to achieve much better momentum resolution close to the design value of 5×10^{-4} for the K1.8 beam line spectrometer calibrated with the S - $2S$. In the Table VI, we used 1×10^{-3} conservatively for the next runs.

Beam time request

After two weeks of beam tune and detector commissioning run, we would like to have the spectrometer tuning run with the scintillation fiber active target to obtain the $p(K^-, K^+)\Xi^-$ reaction data for about five days (30,000 Ξ^- events). We also need calibration runs for the active target by using the K^- beam for a few days. We will irradiate the beam through the whole volume of the scintillation fiber target. In a separated beam period, we would like to take physics data on $^{12}\text{C}(K^-, K^+)\Xi^-$ reaction at 1.8 GeV/c. After a 20-days of running time, we expect to have the number of 110 events in the bound region. It should be noted that the peak counts would be further enhanced owing to the better energy resolution of $S-2S$ by a factor of three (6/2), at least. The flat background events in the pilot run, which is mainly due to π^+ 's from K^- beam decay-in-flight around the target would be suppressed in the $S-2S$ because of the good focusing property of the spectrometer.

6. Summary

In the J-PARC E05 experiment, we aim for establishing the existence of Ξ -hypernuclei as clear peak structures. A new spectrometer $S-2S$ is constructed for the high energy resolution spectroscopy with (K^-, K^+) missing-mass measurement. By combining with an active scintillation fiber target, the energy resolution of better than 2 MeV (FWHM) will be achieved with a thick target of 10 g/cm². The real part and imaginary part of the ΞN potential will be measured in high accuracy.

Here, we would like to propose the following beam time listed in Table VII.

Run	beam time
Detector and Beam Commissioning	≥ 2 weeks
$p(K^-, K^+)\Xi^-$	5 days
Active target calibration	3 days
$^{12}\text{C}(K^-, K^+)\Xi^-$	20 days

Table VII. Beam time request for E05 with $S-2S$ spectrometer.

Detector commissioning and beam tuning runs should be allocated separately from the following runs. Then, after these commissioning, we would like to have calibration data taking for the $p(K^-, K^+)\Xi^-$ reaction and for the active target for 8 day. For both calibration runs we are going to use the fiber scintillation target. At this stage, we might have a short break to analyze the data taken. After confirming the system is working well, we will have the physics data taking by using the fiber scintillation target (10 g/cm²).

In order to perform these data taking, it is crucial that the primary beam power reaches about 100 kW effectively with a new production target and a shorter spill cycle.

References

- [1] H. Tamura *et al.* [J-PARC E13 Collaboration], JPS Conf. Proc. **17**, 011004 (2017).
- [2] H. Takahashi *et al.*, Phys. Rev. Lett. **87**, 212502 (2001).
- [3] J. K. Ahn *et al.* [E373 (KEK-PS) Collaboration], Phys. Rev. C **88**, no. 1, 014003 (2013).
- [4] T. Harada and Y. Hirabayashi, Nucl. Phys. A **759**, 143 (2005).
- [5] K. Sasaki *et al.* [HAL QCD Collaboration], PTEP **2015**, no. 11, 113B01 (2015).
- [6] A. Gal, E. V. Hungerford and D. J. Millener, Rev. Mod. Phys. **88**, no. 3, 035004 (2016).
- [7] P. Demorest, T. Pennucci, S. Ransom, M. Roberts and J. Hessels, Nature **467**, 1081 (2010).
- [8] J. Antoniadis *et al.*, Science **340**, 6131 (2013).
- [9] T. Fukuda *et al.*, Phys. Rev. C **58** (1998) 1306.
- [10] P. Khaustov *et al.*, Phys. Rev. C **61** (2000) 054603.
- [11] M. Kohno and S. Hashimoto, Prog. Theor. Phys. **123** (2010) 157.
- [12] M. Kohno, Phys. Rev. C **81** (2010) 014603.
- [13] K. Nakazawa *et al.*, Prog. Theor. Exp. Phys. **2015** (2015) 033D002.
- [14] T. Gogami *et al.*, Phys. Rev. C **93**, no. 3, 034314 (2016).
- [15] T. Harada, Y. Hirabayashi and A. Umeya, Nucl. Phys. A **914**, 85 (2013).
- [16] C. B. Dover and A. Gal, Ξ *Hypernuclei*, Annals Phys. **146**, 309 (1983).
- [17] T. Gogami, N. Amano, S. Kanatsuki, T. Nagae and K. Takenaka, Nucl. Instrum. Meth. A **817**, 70 (2016).
- [18] L. Tang *et al.* [HKS Collaboration], Phys. Rev. C **90**, no. 3, 034320 (2014).
- [19] T. Motoba *et al.*, Nucl. Phys. A **827** (2009) 318c-320c.